Electronic Supplementary Material (ESI) for Biomaterials Science.

Supporting Information

Stable ratiometric fluorescent probe for hypochlorous acid detection and rheumatoid arthritis evaluation

Liuwei Gu, Yinghao Li, Xiaojie Kong, Ke Zhang, Yuling Qin, Xiaobo Zhou,* Haiwei Ji,* Guo Li* and Li Wu

Nantong Key Laboratory of Public Health and Medical Analysis, School of Public Health, Nantong University, No. 9, Seyuan Road, Nantong 226019, Jiangsu, P. R. China. Email: xbzhou@ntu.edu.cn (X. Zhou); jihaiwei64@ntu.edu.cn (H. Ji); gli@ntu.edu.cn (G. Li).

Table of Contents

1. Experimental Section

Materials and Reagents. Unless otherwise stated, all reagents and chemicals were obtained from commercial suppliers and used without further purification. Fetal bovine serum (FBS), Dulbecco's Modified Eagle Medium (DMEM) were ordered from Gibco. Penicillin/streptomycin, PBS, MTT Cell Cytotoxicity Assay Kit, NO Assay Kit, LPS, were obtained from Beyotime. FITC (Fluorescein 5-isothiocyanate) was obtained from Adamas. NaClO was obtained from Macklin. Poly(5-(2-ethylhexyloxy)-2-methoxy-cyanoterephthalylidene) (CN-PPV) was obtained from Aigma-Aldrich. 4-Aminobenzohydrazide (ABAH), 4-Methoxy-N-(4-methoxyphenyl)-N-(4-(4,4,5,5-tetramethyl-1,3,2-dioxaborolan-2-yl)phenyl)aniline, 4,7-Bis(5-bromo-2-thienyl)-2,1,3-benzothiadiazole and Sodium phosphate dibasic were obtained from Bidepharm. NAC was obtained from KeyGEN BioTECH. PS-PEG-COOH was obtained from Ponsure. (3-Aminopropyl)triethoxysilane (APTES) was obtained from Thermo Fisher. Sodium dihydrogen phosphate dihydrate was obtained from General-reagent.

Cell Cultures. RAW 264.7 cells were incubated on a cell culture plate at 37 ^{o}C with DMEM (10 % FBS and 1 % penicillin-streptomycin).[1]

Animals. Balb/c mice were obtained from the Laboratory Animal Center of Nantong University. All animal experiments were performed under the approval of the Institutional Animal Care and Use Committee.

Characterization. ^{1}H NMR spectra are the results of the Bruker Vance III 400 MHz NMR system at room temperature. The UV-visible absorption spectrum is the result of UV-1900 (Shimadzu, Japan). The fluorescence spectral data are the results measured by the FS5 fluorescence spectrophotometer (Edinburgh, UK). The absorbance of the cells in the 96-well plate is the data read at 570 nm by the Bio-Rad microplate reader. Fluorescence and cell imaging were performed on a Nikon-ti2 inverted microimaging system. Solution phase imaging and mouse knee joint fluorescence imaging were performed on the Small Animal Intravital Imager from Tanon. The size in solution is characterized by dynamic light scattering using the Malvern nano method. The FEI Tecnai F20 high-resolution 200 kV transmission electron microscope (TEM) images

were used. The pH of the solution is adjusted by pH meter.

Materials Synthesis.

The synthetic route of **MeOTPATBT** was shown in Fig S1. The intermediates were carefully prepared according to the literature.[1] Compound **1** ($C_{26}H_{30}BNO_4$, 2.5 eq.) and compound **2** ($C_{14}H_6Br_2N_2S_3$, 1 eq.) were added in toluene (5 mL) with the catalyze of potassium carbonate (2 M), tetrabutylammonium bromide (0.2 eq.), and tetrakis (triphenylphosphine) palladium (0.05 eq.) under the protection of nitrogen. After reaction, the organic phase was washed with dichloromethane and water to afford crude product. The crude product was further purified by silica gel column chromatography using eluent (dichloromethane/petroleum ether, v/v = 1/2) to afford purple solid of acceptor MeOTPATBT ($C_{54}H_{42}O_4N_4S_3$). Compound **1** ($C_{26}H_{30}BNO_4$): 1H NMR (400 MHz, $CDCl_3$), δ (ppm): 7.60 (d = 8 Hz, 2H), 7.06 (d = 8 Hz, 4H), 6.86 (d = 8 Hz, 2H), 6.83 (d = 8 Hz, 4H), 3.80 (s, 6H), 1.32 (s, 12H). compound **2** ($C_{14}H_6Br_2N_2S_3$): 1H NMR (400 MHz, C_7D_8), δ (ppm): 8.16 (s, 1H), 7.79 (d = 4 Hz, 1H), 7.39 (d = 4 Hz, 1H), 7.36 (s, 3H). MeOTPATBT ($C_{54}H_{42}O_4N_4S_3$): 1H NMR (400 MHz, $CDCl_3$), δ (ppm): 8.09 (s, 2H), 7.83 (s, 2H), 7.50 (d = 8 Hz, 4H), 7.08 (d = 12 Hz, 8H), 6.93 (s, 4H), 6.86 (d = 8 Hz, 10H), 3.81 (s, 12H).

The synthetic route of **MeO-CNPPV Pdots** was shown in Fig S5. **MeO-CNPPV Pdots** were synthesized by nanoprecipitation. The polymer CNPPV, PS-PEG-COOH, and small molecule MeOTPATBT were dissolved in anhydrous THF. The concentration of CNPPV, MeOTPATBT was 2 mg/mL. And, the concentration of PS-PEG-COOH was 5 mg/mL. APTES stock solution was diluted 100 times in anhydrous THF. Then 2 μL MeOTPATBT, 200 μL CNPPV, 80 μL PS-PEG-COOH, 10 μL APTES diluent and 108 μL anhydrous THF were uniformly mixed. Under the help of ultrasound, 0.4 mL mixture solution was quickly injected into 2 mL water. THF is removed by heating plate through nitrogen.

Fluorescence spectra of MeO-CNPPV Pdots and their components. 200 μg/mL of **MeO-CNPPV Pdots** stock solution and 2 mg/mL of CNPPV and MeoTPATBT mother liquor were diluted to 10 μg/mL in PB (pH 7.4), and absorption and emission spectra were recorded with a UV-VIS spectrometer and fluorescence spectrometer in 25 ^oC.

Stability test of MeO-CNPPV Pdots. 0.2 mol/L NaH_2PO_4 and 0.2 mol/L Na_2HPO_4 were mixed by pH meter to prepare 0.2 mol/L phosphate buffer (PB) with different pH (pH = 5, 6, 7, 8, 9). Select the PB solution with the optimal pH (pH 7.4), conFig the probe solution with 10 μg/mL, and heat the water bath to different temperatures to observe the change of absorption spectrum and emission spectrum. In the optimal pH (pH 7.4) and the optimal temperature (25 ^oC) environment, the probe solution of 10 μg/mL was continuously illuminated to observe the changes of absorption and emission spectra in different time periods. The APTES stock solution was diluted into the 1 % reserve solution. In the optimal environment, two groups of 10 μg/mL probe solutions, one containing 10 μL APTES diluent and the other the blank sample, were configd to record the emission spectrum changes at 600 nm and 680 nm by fluorescence spectrometer.

Quantum yield measurement of MeO-CNPPV Pdots. By using FITC in PBS (QY = 0.91) as reference fluorophore to measure the quantum yield of fluorophores. Ex = 440 nm. The quantum yield was calculated in the following manner.[2]

$$\phi = \phi_{ref} \times (n^2_{sample} / n^2_{ref}) (I_{sample} / A_{sample}) (A_{ref} / I_{ref})$$

Maintain the absorbance of different concentration gradients at or below 0.1 and detect the corresponding fluorescence spectra. Calculate the fluorescence integral area. The integral area of the 450-610 nm and 610-800 nm region represents the 600 nm and 680 nm channel, respectively. The scalar curves were plotted by integrating fluorescence and absorbance, and the quantum yields of MeO-CNPPV Pdots before and after reaction with ClO^- at two-channel were calculated by slope comparison.

Spectra Responses of MeO-CNPPV Pdots and CNPPV to ClO^-. The NaClO solution (800 μM) was prepared with sodium hypochlorite (≥ 60 %). **MeO-CNPPV Pdots** stock and NaClO solution were mixed in PB (pH 7.4) at a final concentration of 10 μg/mL **MeO-CNPPV Pdots** and 200 μM NaClO to detect the time-dependent fluorescence spectrum of samples at 600 nm and 680 nm. The **MeO-CNPPV Pdots** stock solution and NaClO solution were prepared into a 2 mL system with PB (pH 7.4). The final concentration of **MeO-CNPPV Pdots** was 10 μg/mL, and that of NaClO was 0, 1, 2, 3, 4, 6, 7, 8, 10, 12, 14, 16, 18, 20, 22, 24, 26, 28, 30, 40, 50, 60, 70 and 80 μM, respectively. The

fluorescence intensity of the samples was examined after incubation at 25 °C for 5 min. Scatter plots and line plots were drawn based on the fluorescence ratios at 600 nm and 680 nm from 0-80 μM and 3-16 μM, respectively, and the detection limit was calculated. Similarly, the fluorescence spectra of CNPPV mixed with NaClO solutions of different concentrations were tested. Meanwhile, detect a solution of **MeO-CNPPV Pdots** mixed with 50 μM NaClO for a clear contrast.

Fluorescence imaging of MeO-CNPPV Pdots in response to ClO^- in the solution phase. A mixture of 300 μL **MeO-CNPPV Pdots** and NaClO was added to the 96-well plate, with **MeO-CNPPV Pdots** (10 μg/mL), and NaClO at different concentrations (0, 4, 8, 16, 32, 64 μM).[3] Subsequently, fluorescence imaging was performed in a small animal live imager with blue excitation light source and filters of 690 ± 25 and 605 ± 35. Draw the fluorescence quantification histograms and calculate the I_{600}/I_{680} ratio and plot the ratio image from the fluorescence intensity.

Selectivity Detection. The interfering ion mother liquor (Na_2SO_4, NaCl, $NaNO_2$, $AlCl_3$, $CaCl_3$, $FeSO_4$, $CuCl_2$, $ZnCl_2$, GSH, $Na_2S_2O_3$, $FeCl_3$, $FeCl_2$, $MgCl_2$, KCl, Cys, $NaHSO_4$, H_2O_2, $^1O_2$, ·OH, $O_2^{\cdot-}$, $ONOO^-$, NO, NaF, Cl^-, OH^-, HCO_3^-)[4] with concentration of 0.1 M and the NaClO mother liquor with concentration of 1 mM were prepared. Among them, $ONOO^-$ quantified by absorption, quantitative formula is C (mM) =Abs (at absorption peak = 302 nm) / 1.67. $O_2^{\cdot-}$ quantified by absorption, quantitative formula is C (mM) =Abs (at absorption peak = 250 nm) / 2.682. NO quantified by NO assay kit. A 2 mL mixed solution containing various interfering ions, **MeO-CNPPV Pdots**, was prepared by PB (pH 7.4). The solubility of interference ion is 100 μM, the concentration of probe is 5 μg/mL, and the concentration of ClO^- is 100 μM. After incubation at 25 °C for 5 min, the fluorescence intensity of the sample was detected and fluorescence quantitative histogram and ratiometric value ($I_{600\ nm}/I_{680\ nm}$) diagram were drawn.

The stability of MeO-CNPPV Pdots in DMEM including 10% FBS. MeO-CNPPV Pdots incubated with DMEM and cells for 24h before entering the cells. Therefore, the fluorescence stability of **MeO-CNPPV Pdots** (10 μg/mL) in DMEM within 30 h was measured. DMEM has two emission peaks at 510 nm and 590 nm, and the intensity of

these two emission peaks is subtracted during fluorescence quantitative analysis of **MeO-CNPPV Pdots.**

MTT experiment. RAW 264.7 cells, HepG2 cells and MCF-7 cells were incubated in a 96-well cell culture plate with 1.5 × 10^4 cells per well and incubated in humid atmosphere (5 % carbon dioxide) at 37 ^oC for 24 h. Removing culture medium, and adding 100 μL of different concentrations of **MeO-CNPPV Pdots** solution (0, 5, 10, 20, 30, 40, 50, 60, 80 μg/mL) composed of DMEM (10 % fetal bovine serum, 1 % antibiotic) to each well, and then cultured in the same environment for 25 h. Then, adding 10 μL of MTT solution to each well. After the cells were incubated for 4 h, 100 μL formazan solvent zan solvent was added to each well to dissolve purple formazan. Finally, the absorbance of 490 nm was measured with an enzymoleter, and cell viability was calculated using the following equation: Cell viability (%) = (mean of Abs. value of treatment group/mean Abs. value of control) × 100 %.

Detection of endogenous and exogenous ClO^- in RAW 264.7. Cells are collected during the exponential phase of growth. RAW 264.7 cells were rinsed with PBS and then digested with 2 mL trypsin-EDTA solution (0.25 w/v % trypsin, 2.5 g/L EDTA) at 37 ^oC for 2 min. The suspended cell solution was collected and centrifuged, and the culture medium was discarded after the centrifugation. The suspension was remade with DMEM medium and counted under a microscope. Then 1 × 10^5 RAW 264.7 cells were inoculated in confocal petri dishes and incubated with 10 μg/mL **MeO-CNPPV Pdots** for 25 h in a humid environment (5 % CO_2) at 37 ^oC. Prior to fluorescence imaging, cells were washed twice with PBS solution to remove Pdots non-specific on the cell membrane. To detect exogenous ClO^-, RAW 264.7 cells pretreated with **MeO-CNPPV Pdots** were incubated at 37 ^oC for 30 min in PBS solution (pH 7.4) containing different concentrations of NaClO (0, 5, 10, 15, 30). The cells were washed three times with 1× PBS (pH 7.4) buffer before imaging.

In order to detect the endogenous ClO^- of RAW 264.7 cells, the exponential stage cells were inoculated into glass-bottom culture dishes and divided into 12 groups. In advance, 10 μg/mL **MeO-CNPPV Pdots**, 10 μg/mL LPS, 5 μM NAC and 250 μg/mL ABAH were prepared with DMEM.[5] After the cells were completely attached to the wall, 1

mL of prepared NAC (5 μM) and ABAH (250 μg/mL) solutions were added into the cells of the ABAH and NAC groups, and incubated for 1 h as the negative control group. 1 mL of prepared LPS (10 μg/mL) solution was added into the cells of the two groups of LPS groups and incubated for 0.5 h as the positive control group. At the same time, two other groups of cells pretreated with NAC (5 μM) and ABAH (250 μg/mL) were added to 1 mL prepared LPS (10 μg/mL) solution and incubated for 0.5 h. In addition, 1 mL NAC (5 μM) and 1 mL ABAH (250 μg/mL) were added to the two groups of cells pretreated with LPS (10 μg/mL) for 1 h, respectively, as the treatment group. After incubation in all groups, 1 mL of 10 μg/mL **MeO-CNPPV Pdots** solution was added and incubated for 25 h until Pdots entered the cells. In the control experiment, the cells were incubated only with **MeO-CNPPV Pdots** (10 μg/mL) for 25 h. **MeO-CNPPV Pdots** are not added to the Blank group. Cells were washed 3 times with 1× PBS solution before imaging.

Intracellular photostability imaging of MeO-CNPPV Pdots. 1×10^5 RAW 264.7 cells were inoculated in confocal petri dishes and incubated with 10 μg/mL Rhodamine 110, Rubrene and **MeO-CNPPV Pdots** for 25 h in a humid environment (5 % CO_2) at 37 ^oC. Prior to fluorescence imaging, cells were washed twice with PBS solution to remove Pdots non-specific on the cell membrane. RAW 264.7 cells pretreated with **MeO-CNPPV Pdots** were incubated at 37 ^oC for 30 min in PBS solution (pH 7.4) containing different concentrations of NaClO (0, 50 μM). The cells were washed three times with 1× PBS (pH 7.4) buffer before imaging. The cells were irradiated for 10 minutes and a fluorescence image was obtained every two minutes. Quantitative analysis was performed according to cell fluorescence imaging.

Fluorescence imaging experiments were performed using a Nikon inverted microscope capturing fluorescence images of cells with a 60X/oil objective and excitation wavelength of 480 ± 25 nm or 425 ± 25 nm. The fluorescence emission at the emission filter 535 ± 45 nm, 690 ± 25 and 605 ± 35, respectively. 600 and 680 nm is collected through two-channel: BP 605 ± 35 and BP 690 ± 25 (BP means "band pass", anything between the indicated wavelengths can be passed). Image processing and analysis were performed on the Image J software.

Inflammation models.[6] In order for **MeO-CNPPV Pdots** to be effective in vivo, the optimal concentration needs to be selected. **MeO-CNPPV Pdots** were prepared into solutions of different concentrations (0.2, 0.4, 0.6, 0.8, 1.0, 1.2, 1.4, 1.6 μg/mL) in 0.5 mL EP tubes and then imaged on a small animal live imager. We demonstrated the feasibility of **MeO-CNPPV Pdots** imaging ClO^- in a BALB/c mouse model with early arthritis phenotype.[7] First, LPS (10 mg/mL, 25 μL) of two groups of BALB/c mice (3 mice per group) was induced by arthritis under anesthesia (3 days after injection). Subsequently, NAC (60 mg/mL, 25 μL) was injected into the tail vein of one group of LPS-pretreated mice for 3 days, and **MeO-CNPPV Pdots** (8 μg/mL) were injected into the right joint of the mice on the 7th day, and fluorescence imaging was performed 10 min later. Control mice were injected with saline at the joints for the first three days, and imaging was performed on the seventh day. The excitation light is blue and the emission wavelength is collected with BP 605 ± 35 and BP 690 ± 25 filters. Image processing and fluorescence intensity analysis were carried out on Image J software.

2. Supporting Figs

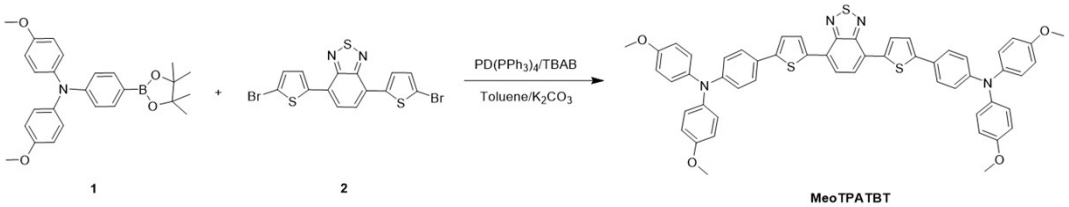

Fig S1. Synthetic route of **MeoTPATBT**.

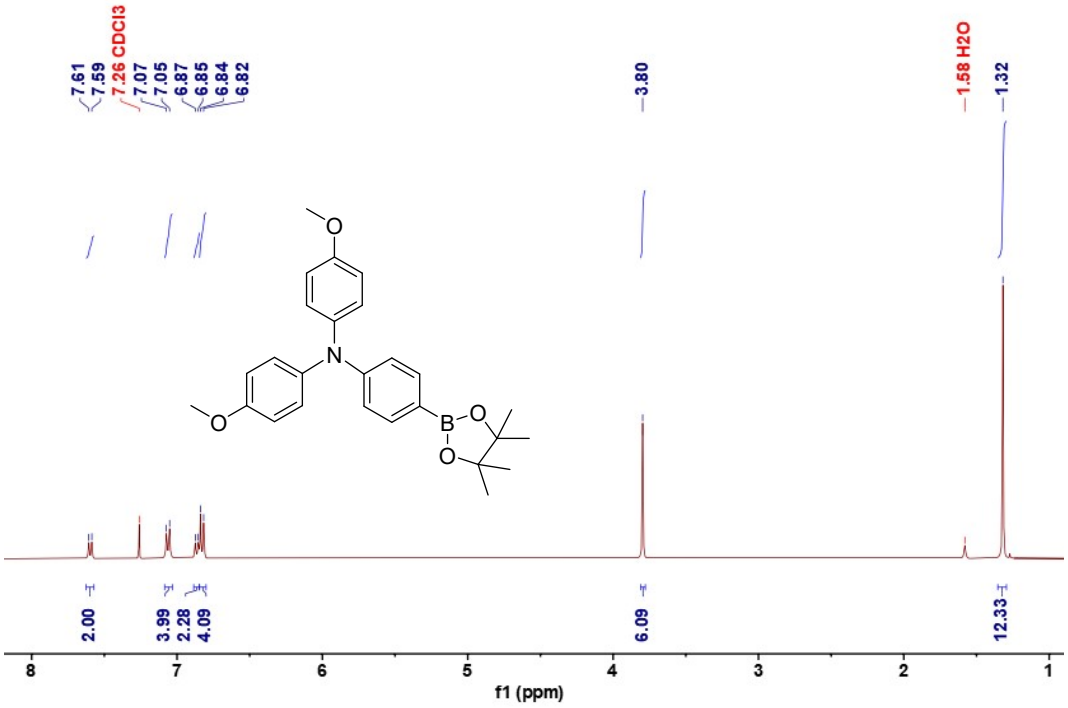

Fig S2. ^{1}H NMR spectrum of compound **1** in $CDCl_3$.

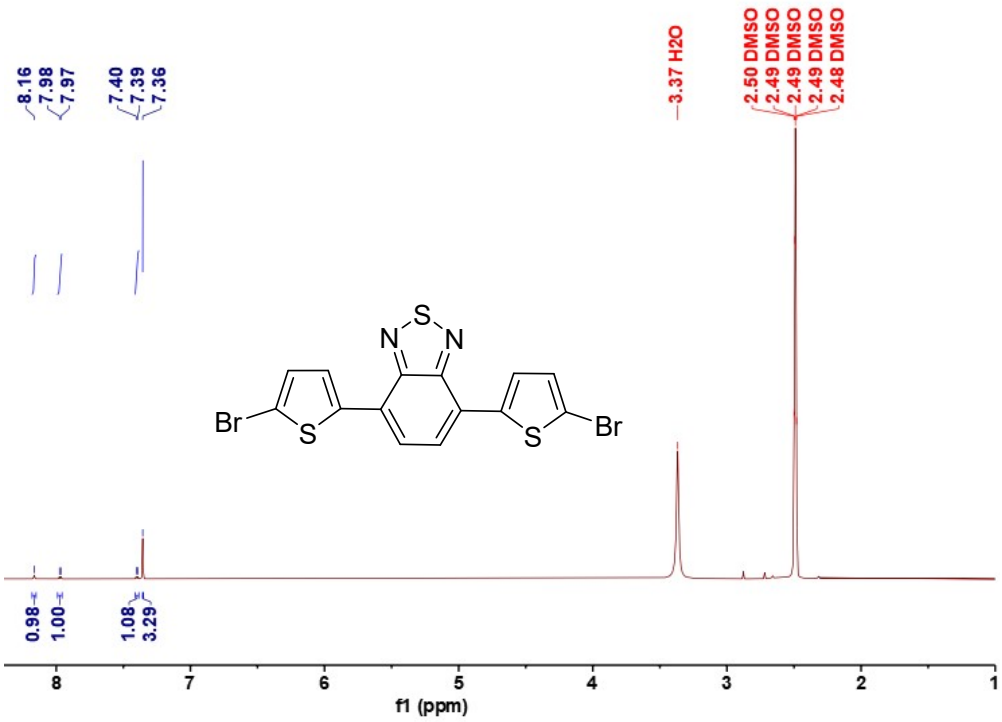

Fig S3. ^{1}H NMR spectrum of compound **2** in Toluene-d8.

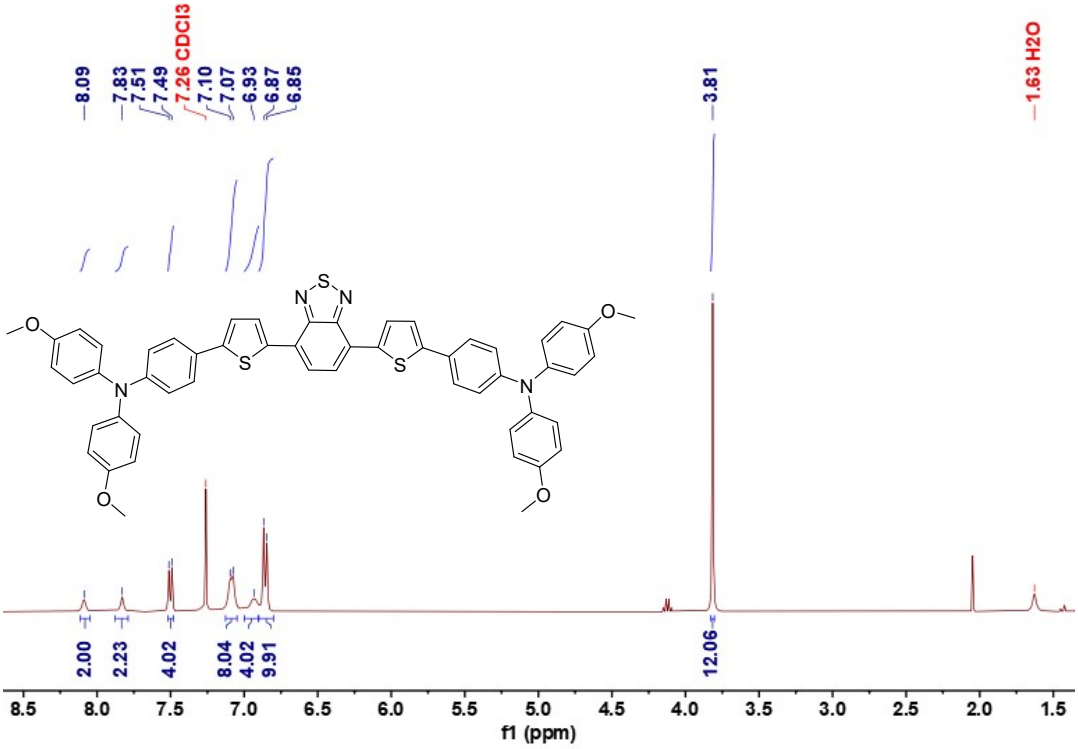

Fig S4. ^{1}H NMR spectrum of **MeOTPATBT** in $CDCl_3$.

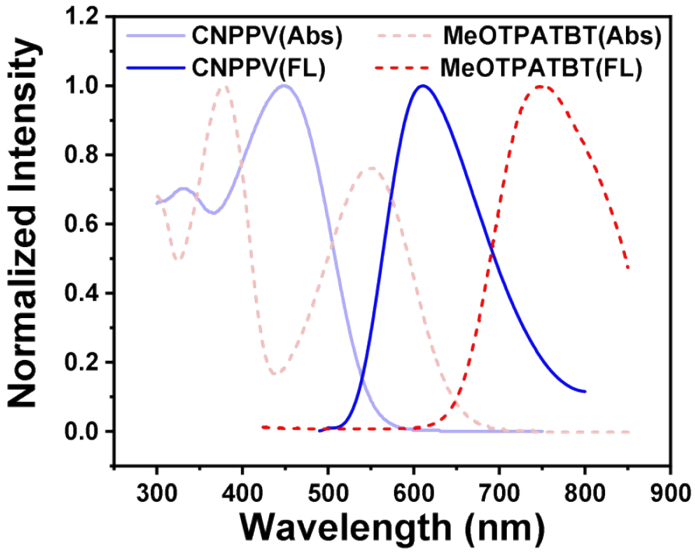

Fig S5. Normalized absorption and emission spectra of CNPPV as well as MeOTPATBT.

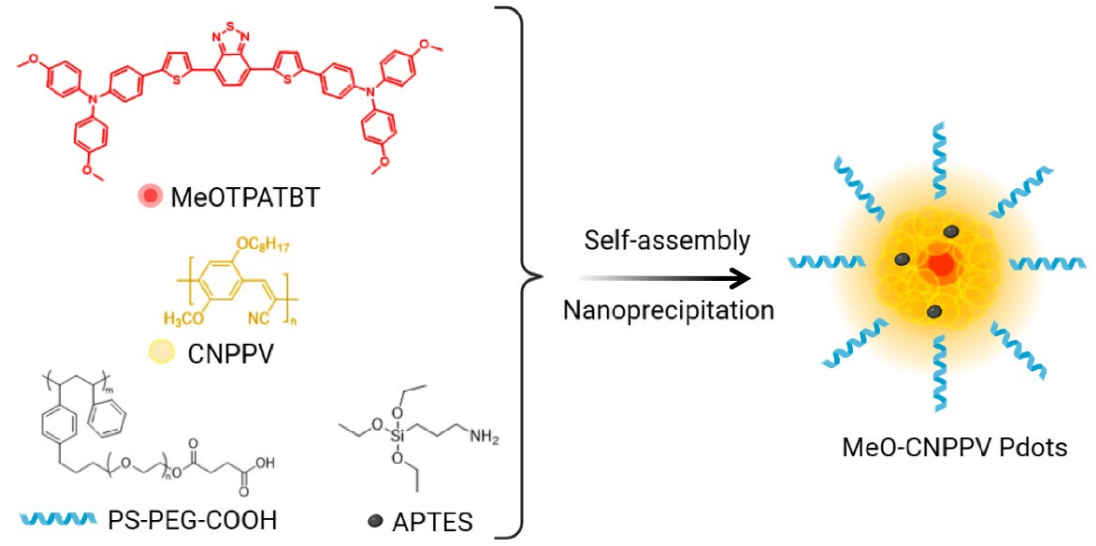

Fig S6. Synthetic route of **Meo-CNPPV Pdots**.

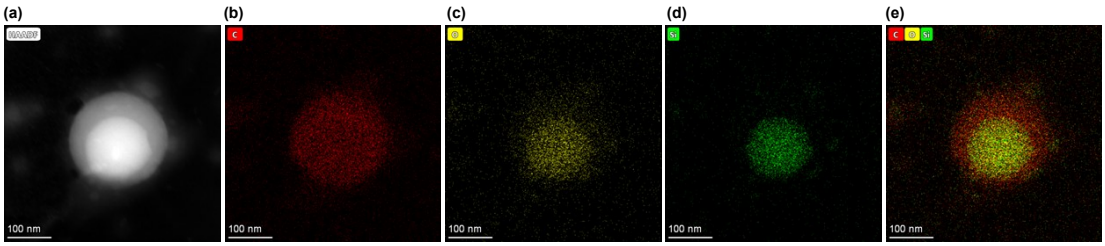

Fig S7. (a) High-angle annular dark field imaging (b) carbon, (c) oxygen, (d)silicon analysis and (e) merge imageing of **MeO-CNPPV Pdots**.

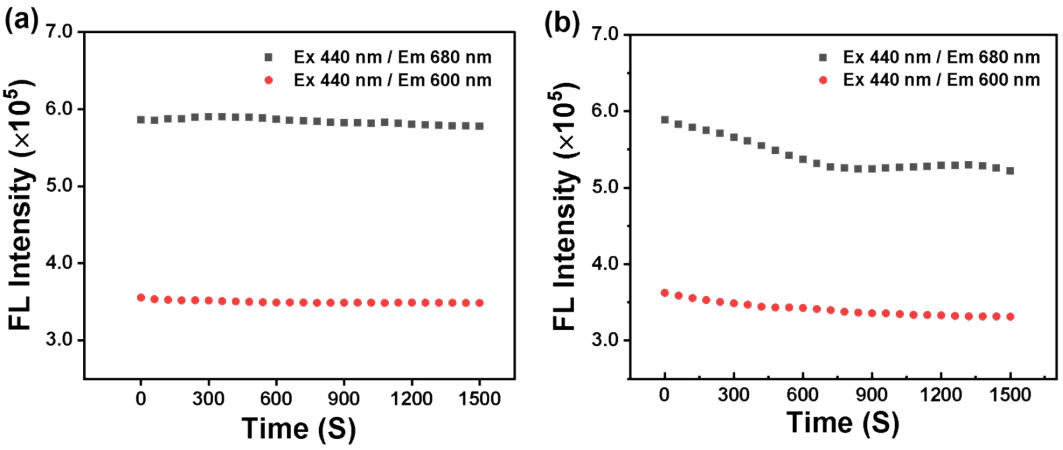

Fig S8. Fluorescence spectra of **MeO-CNPPV Pdots** solution (10 μg/mL) (a) with APTES and (b) without APTES.

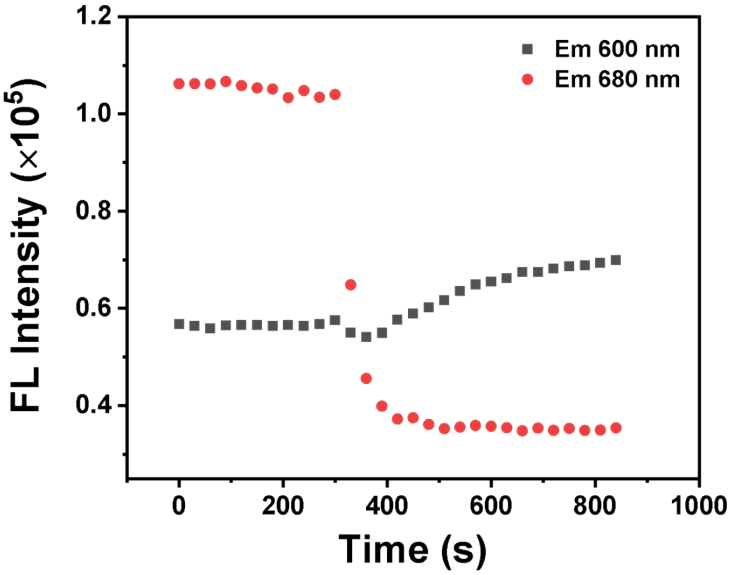

Fig S9. Photostability of **MeO-CNPPV Pdots** (10 μg/mL) at 600 nm and 680 nm under the concentration of ClO^- (200 μM).

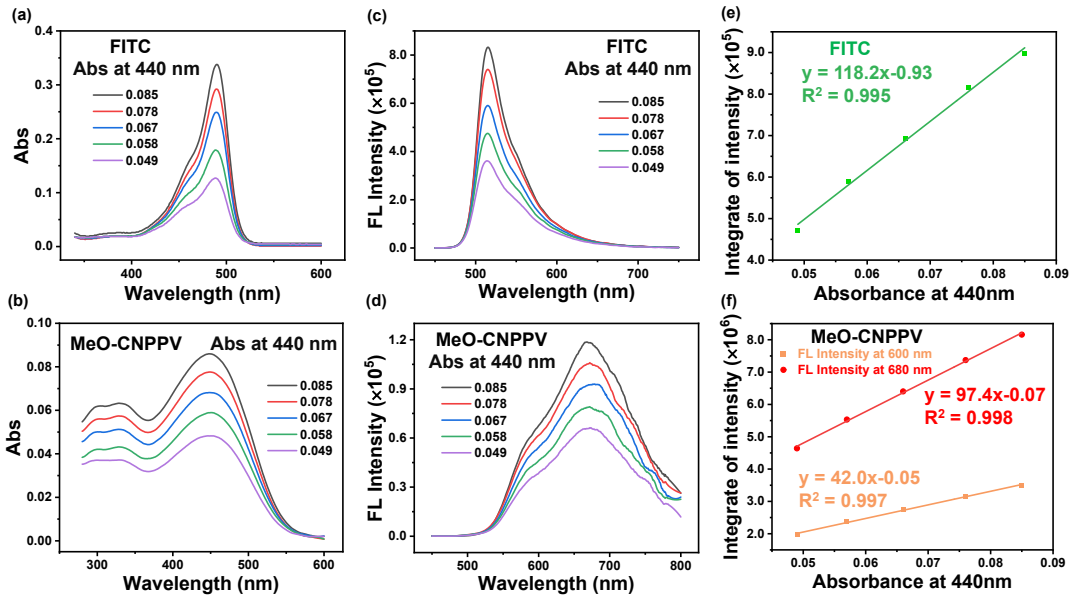

Fig S10. Fluorescence quantum yield measurement of reference fluorophores (FITC) and **MeO-CNPPV Pdots** before reaction with ClO^- in PBS. Absorption spectra of different concentrations of (a) FITC and (b) **MeO-CNPPV Pdots** in PBS. Fluorescence spectra of (c) FITC and (d) **MeO-CNPPV Pdots** with different concentrations respectively corresponded with a) and b). Excitation wavelength: 440 nm. (e) Integrated fluorescence intensity drew as a function of absorbance at 440 nm for FITC solutions based on the measurements in a) and c). The data was fitted into a linear function with a slope of 118.2. (f) Integrated fluorescence intensity of two-channel (450-610 nm and 610-800 nm) drew as a function of absorbance at 440 nm for **MeO-CNPPV Pdots** solutions based on the measurements in b) and d). The data was fitted into a linear function with a slope of 42.0 and 97.4, respectively.

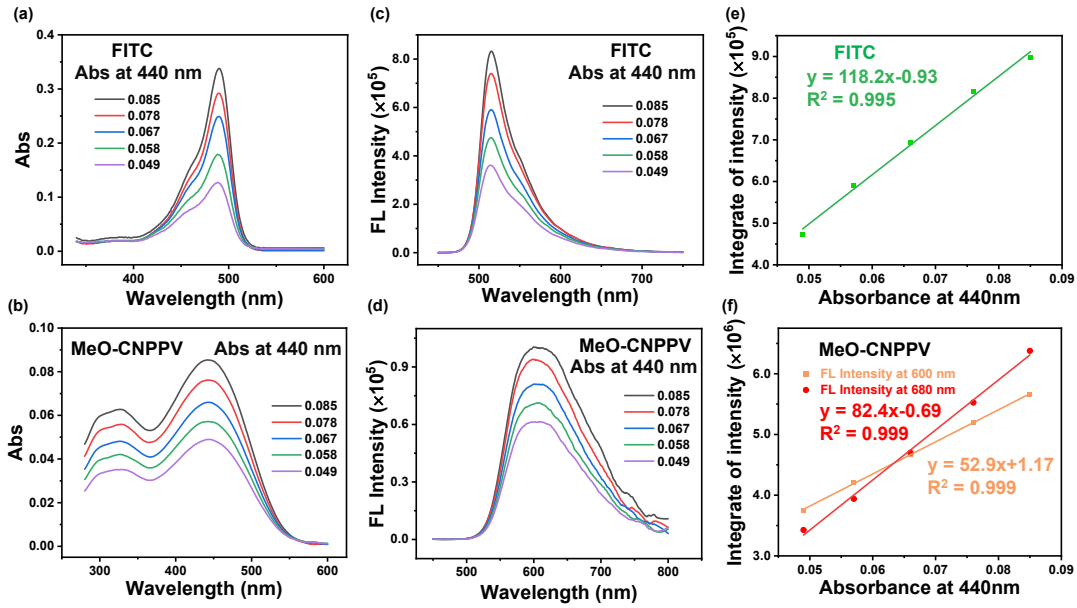

Fig S11. Fuorescence quantum yield measurement of reference fluorophores (FITC) and **MeO-CNPPV Pdots** after reaction with ClO^- in PBS. Absorption spectra of different concentrations of (a) FITC and (b) **MeO-CNPPV Pdots** in PBS. Fluorescence spectra of (c) FITC and (d) **MeO-CNPPV Pdots** with different concentrations respectively corresponded with a) and b). Excitation wavelength: 440 nm. (e) Integrated fluorescence intensity drew as a function of absorbance at 440 nm for FITC solutions based on the measurements in a) and c). The data was fitted into a linear function with a slope of 118.2. (f) Integrated fluorescence intensity of two-channel (450-610 nm and 610-800 nm) drew as a function of absorbance at 440 nm for **MeO-CNPPV Pdots** solutions based on the measurements in b) and d). The data was fitted into a linear function with a slope of 52.9 and 82.4, respectively.

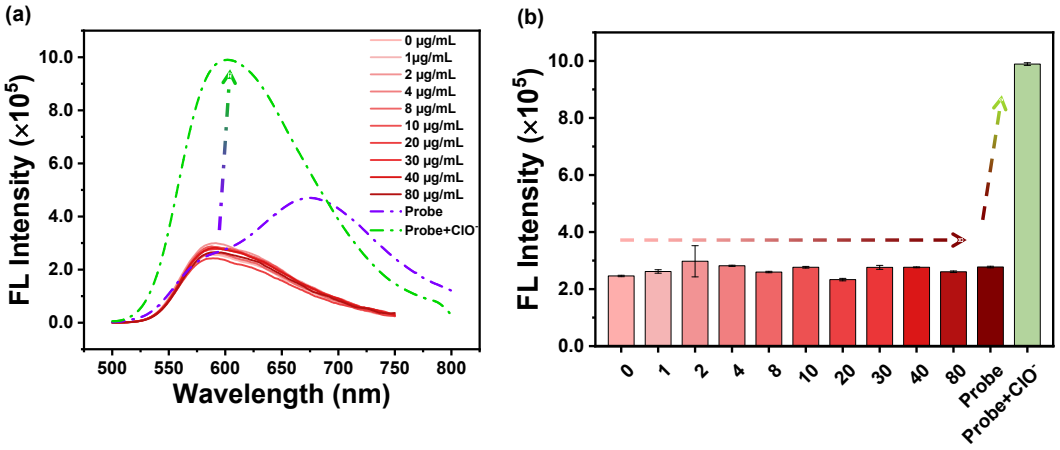

Fig S12. The fluorescence performance of CNPPV in the presence of different concentrations of NaClO solutions. (a) Fluorescence spectra and (b) quantification of fluorescence intensity of CNPPV treated with different concentrations of 1, 2, 4, 8, 10, 20, 30, 40, 80 μg/mL. For contrast, the fluorescence performance of **MeO-CNPPV Pdots** after reaction with ClO^- was detected.

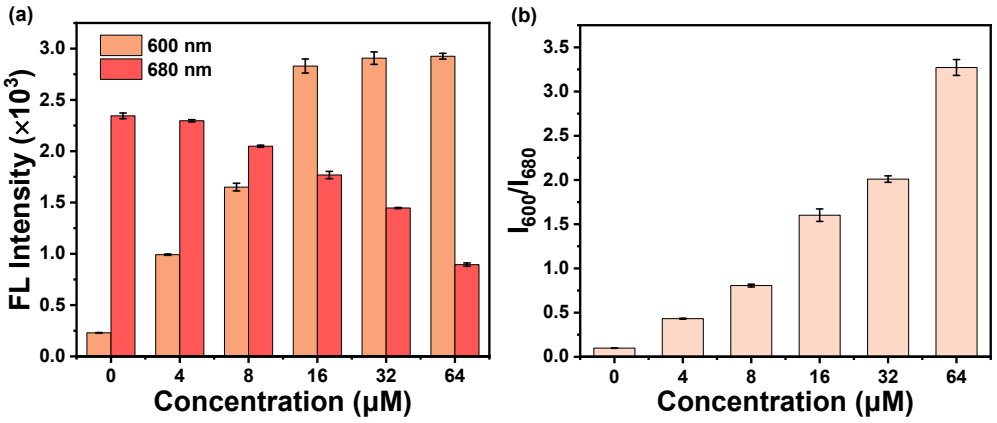

Fig S13. (a) Fluorescence quantification and (b) ratiometric value ($I_{600\ nm}/I_{680\ nm}$) of **MeO-CNPPV Pdots** with different concentrations of NaClO solutions.

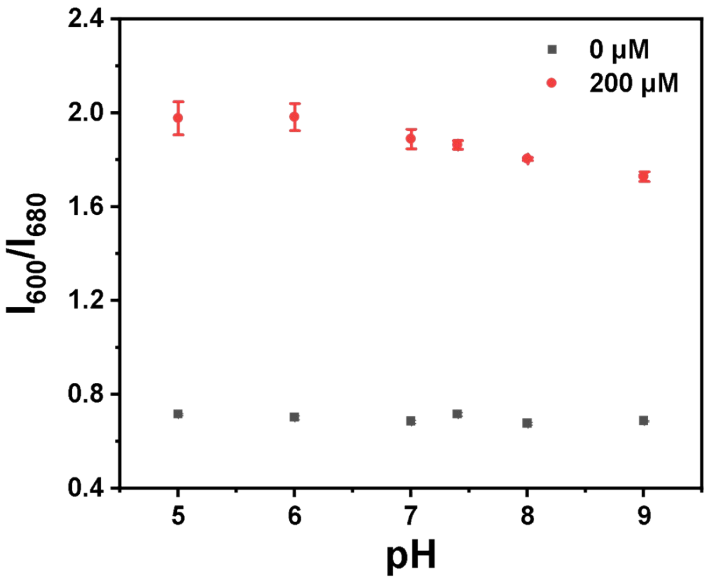

Fig S14. Fluorescence ratiometric value ($I_{600\ nm}/I_{680\ nm}$) of **MeO-CNPPV Pdots** in 0 μM and 200 μM NaClO solutions under different pH values.

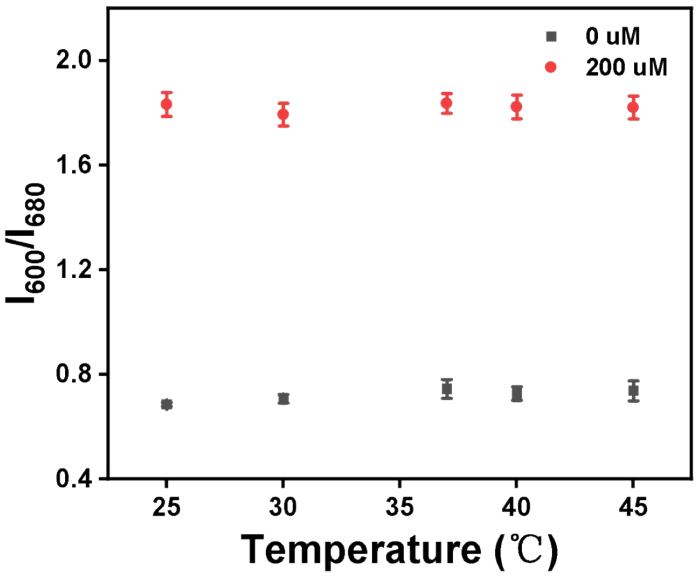

Fig S15. Fluorescence ratiometric value ($I_{600\ nm}/I_{680\ nm}$) of **MeO-CNPPV Pdots** in 0 μM and 200 μM NaClO solutions under different temperature.

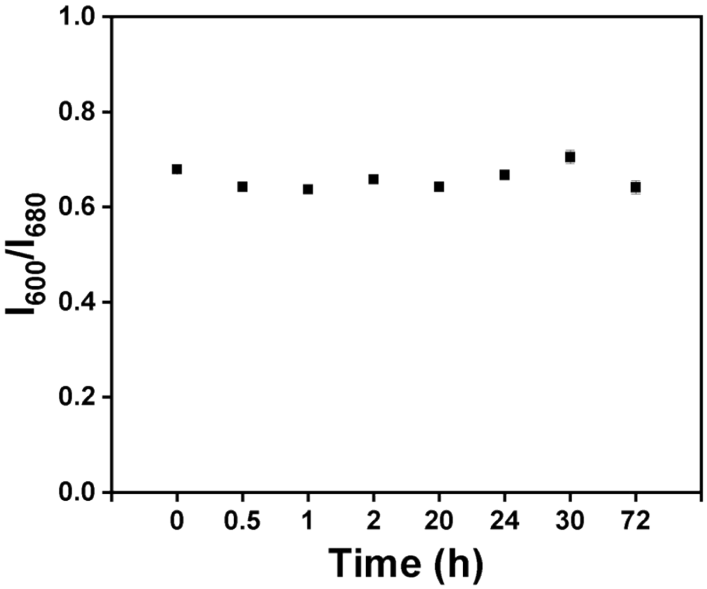

Fig S16. The fluorescence ratio ($I_{600\ nm}/I_{680\ nm}$) of **MeO-CNPPV Pdots** (10 μg/mL) without protecting from light within 72 h.

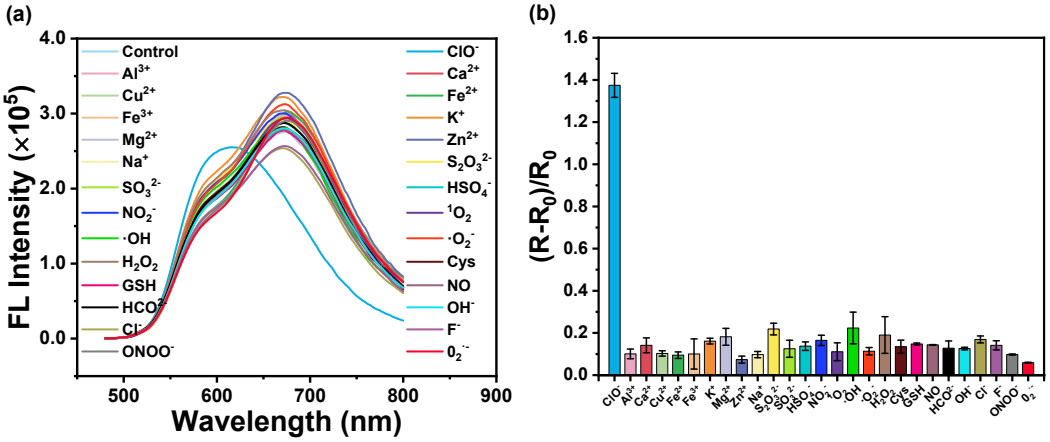

Fig S17. (a) Fluorescence spectra and (b) fluorescence ratiometric value ($(R-R_0)/R_0$) of **MeO-CNPPV Pdots** (5 μg/mL) for different interfering ions (100 μM).

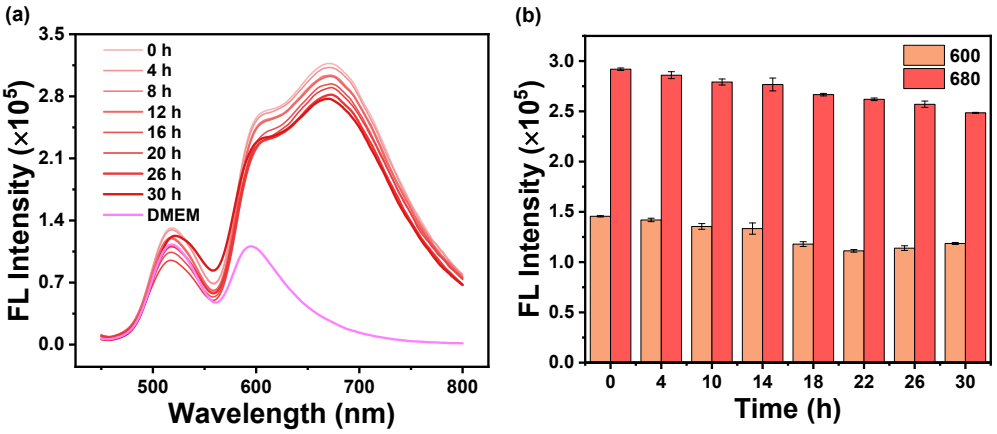

Fig S18. The stability of **MeO-CNPPV Pdots** in DMEM including 10% FBS. (a) Fluorescence spectra of DMEM and **MeO-CNPPV Pdots** within 30 h. (b) Quantification of fluorescence intensity of **MeO-CNPPV Pdots** at 600 nm and 680 nm through subtracting the fluorescence value of DMEM.

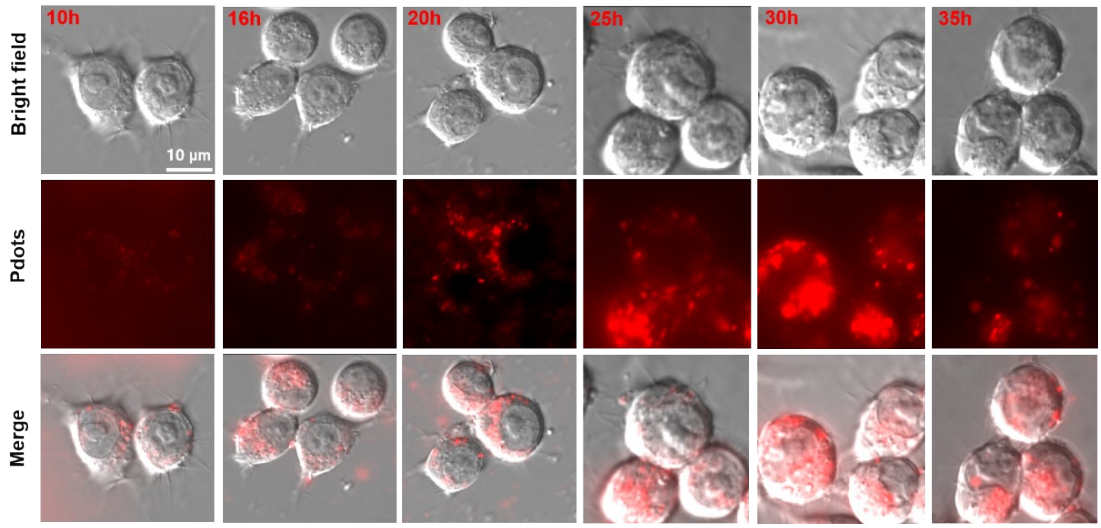

Fig S19. Fluorescence microscopy images of **MeO-CNPPV Pdots** (10 μg/mL) at 680 nm with time increasing in RAW 264.7 cells. Emission wavelength: 680 nm. Scale bar: 10 μm.

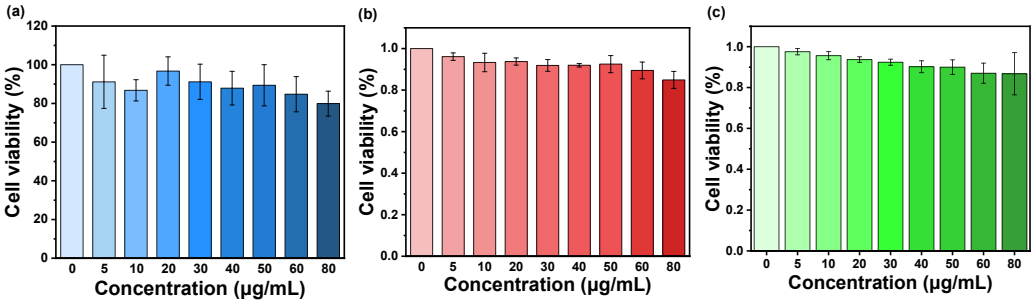

Fig S20. Cytotoxicity research of **MeO-CNPPV Pdots**. In vitro viability of (a) RAW 264.7 cells, (b) HepG2 cells and (c) MCF-7 cells treated with different concentrations of 5, 10, 20, 30, 40, 50, 60, 80 μg/mL for 24 h.

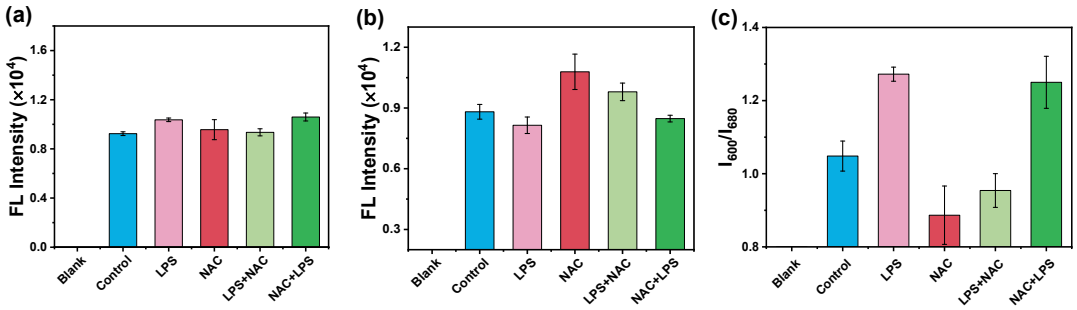

Fig S21. Fluorescence quantification at (a) 600 nm and (b) 680 nm and (c) ratiometric value ($I_{600\ nm}/I_{680\ nm}$) of endogenous ClO^- with NAC as ROS scavengers in RAW 264.7 cells.

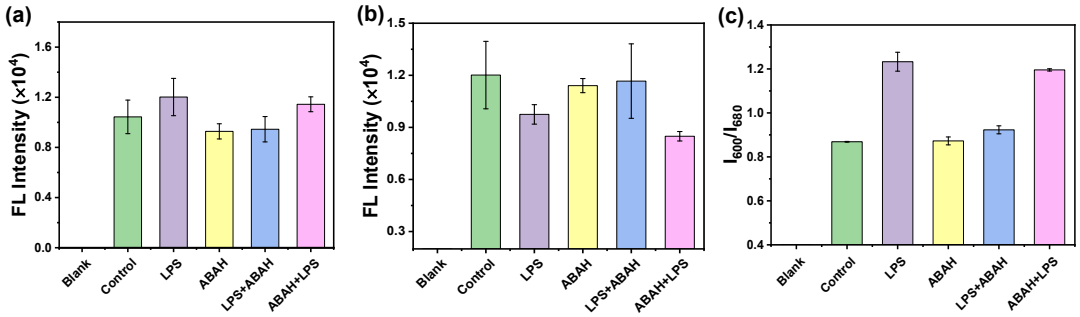

Fig S22. Fluorescence quantification at (a) 600 nm and (b) 680 nm and (c) ratiometric value ($I_{600\ nm}/I_{680\ nm}$) of endogenous ClO^- with ABAH as ROS scavengers in RAW 264.7 cells.

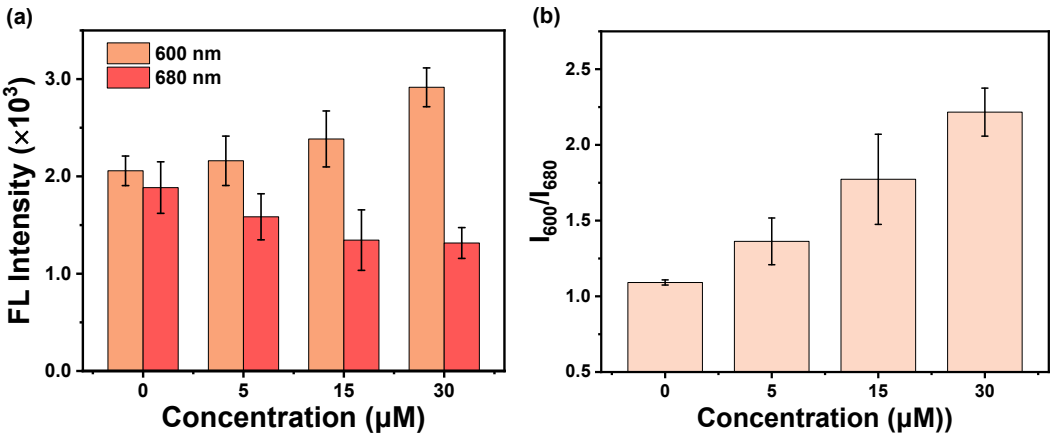

Fig S23. (a) Fluorescence quantification of exogenous ClO^- in RAW 264.7 cells at 680 nm and 600 nm. (b) Fluorescence ratiometric value ($I_{600\ nm}/I_{680\ nm}$) of exogenous ClO^-.

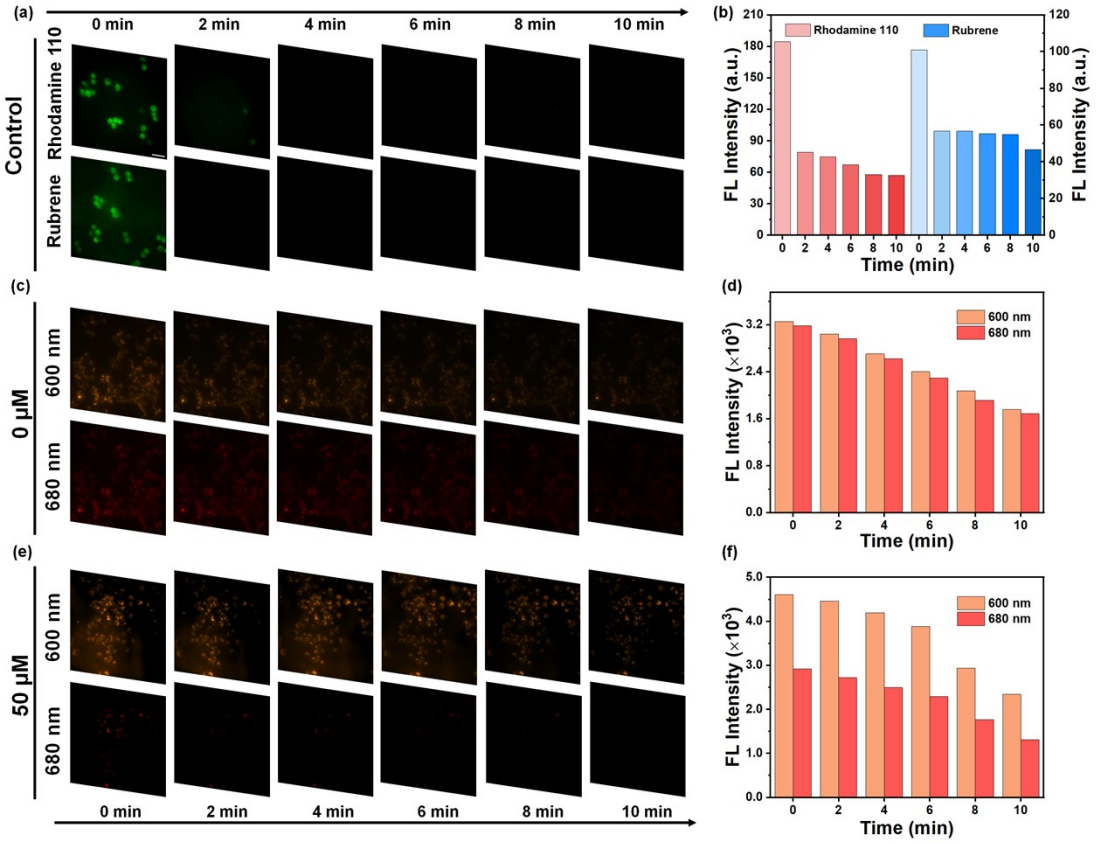

Fig S24. Intracellular photostability imaging at 600 nm and 680 nm within 10 minutes of (a) Rhodamine 110 and Rubrene after reaction with exogenous ClO^- 50 μM. (b) Quantification of fluorescence intensity of the fluorescence imaging. Intracellular photostability imaging at 600 nm and 680 nm within 10 minutes of **MeO-CNPPV Pdots** after reaction with exogenous ClO^- with (c) 0 μM and (e) 50 μM. Quantification of fluorescence intensity of the fluorescence imaging with (d) 0 μM ClO^- and (f) 50 μM ClO^-.

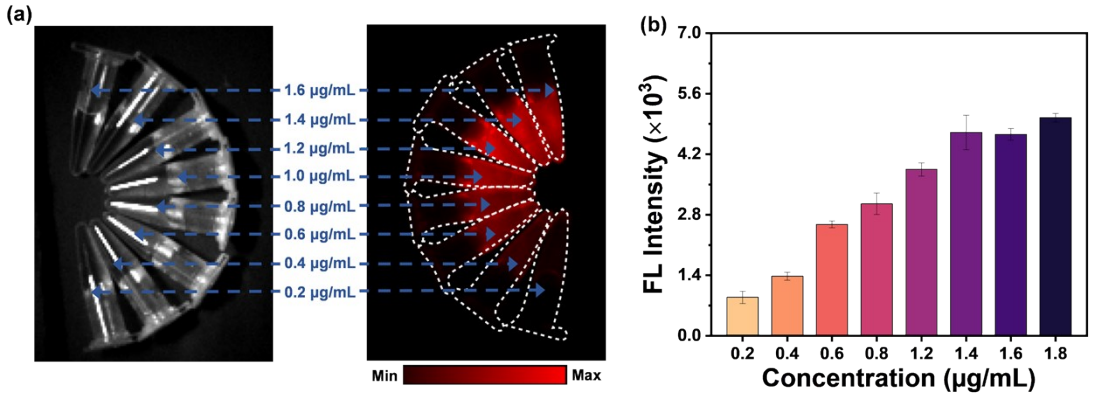

Fig S25. (a) Bright field, fluorescence images and (b) fluorescence quantification of **MeO-CNPPV Pdots** nanoprobe solution at different concentrations. Emission wavelength: 680 nm.

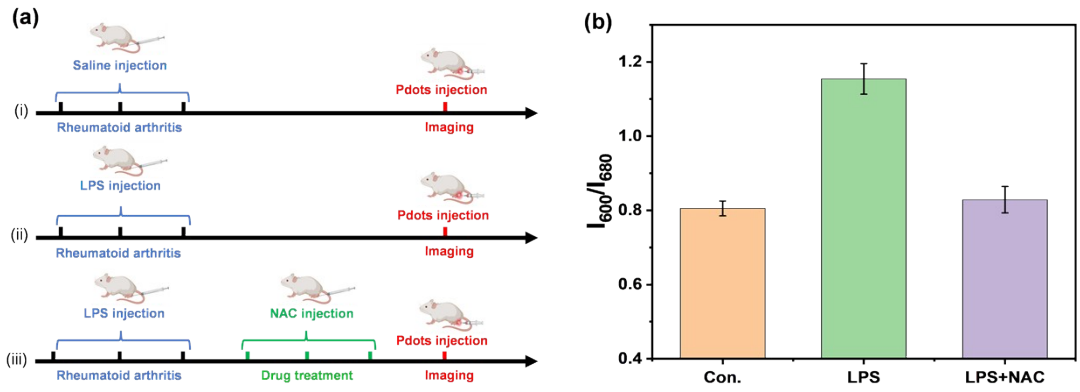

Fig S26. (a) Schematic diagram of arthritis induction and treatment options. (b) Fluorescence ratiometric value ($I_{600\ nm}/I_{680\ nm}$) of the knee joint of RA mice after injection of **MeO-CNPPV Pdots**. Data were presented as the mean ± sd (n = 3).

Table S1. Quantum yield (QY) characterizations of **MeO-CNPPV Pdots**.

Different modes	QY
pure probe (450-610nm)	0.32
pure probe (610-800nm)	0.74
pure probe + 80 μM NaClO (450-610nm) ↑	0.40
pure probe + 80 μM NaClO (610-800nm) ↓	0.63

3. References

1. Y. Li, L. Scudiero, T. Ren and W. Dong, *J. Photochem. Photobiol. A*, 2012, **231**, 51-59.
2. X. Zhou, K. Zhang, C. Yang, Y. Pei, L. Zhao, X. Kang, Z. Li, F. Li, Y. Qin and L. Wu, *Adv. Funct. Mater.*, 2022, **32**, 2109929.
3. X. Ge, Y. Lou, L. Su, B. Chen, Z. Guo, S. Gao, W. Zhang, T. Chen, J. Song and H. Yang, *Anal. Chem*., 2020, **92**, 6111-6120.
4. D. Li, S. Wang, Z. Lei, C. Sun, A. M. EI-Toni, M. S. Alhoshan, Y. Fan and F. Zhang, *Anal. Chem.*, 2019, **91**, 4771-4779.
5. X. Wang, R. Wang, Q. Ding, W. Wu, F. Che, P. Li, W. Zhang, W. Zhang, Z. Liu, and B. Tang, *Anal. Chem*., 2022, **94**, 9811-9818.
6. X. Meng, Y. Shi, Z. Chen, L. Song, M. Zhao, L. Zou, S. Liu, W. Huang, and Q. Zhao, *ACS Appl. Mater. Interfaces*., 2018, **10**, 35838-35846.
7. S. Zhang, L. Ning, Z. Song, X. Zhao, F. Guan, X. Yang, and J. Zhang, *Anal. Chem.*, 2022, **94**, 5805-5813.